Mechanical property and conductivity of a flax fibre weave strengthened magnetorheological elastomer

2017 Smart Mater. Struct. 26 075013

(http://iopscience.iop.org/0964-1726/26/7/075013)

IOP Publishing Smart Materials and Structures
Smart Mater. Struct. **26** (2017) 075013 (12pp) https://doi.org/10.1088/1361-665X/aa73fc

Mechanical property and conductivity of a flax fibre weave strengthened magnetorheological elastomer

Xinglong Gong[1], **Yu Wang, Tao Hu and Shouhu Xuan**[1]

CAS Key Laboratory of Mechanical Behavior and Design of Materials, Department of Modern Mechanics, University of Science and Technology of China, Hefei 230027, People's Republic of China

E-mail: gongxl@ustc.edu.cn and xuansh@ustc.edu.cn

Received 15 March 2017, revised 20 April 2017
Accepted for publication 18 May 2017
Published 14 June 2017

Abstract

This work reported a novel flax-fibre-weaves (FFWs) incorporated magnetorheological elastomer (MRE), whose shear properties, compressive properties, tensile properties, and electrical performance were critically increased by the FFWs. In comparison to the pure MRE, the plastic deformation of the FFW–MRE was smaller and it absorbed more energy under the quasi-static compression and tension. With increasing of the FFW from 1 to 2 and 3 layers, the tensile strength of the MRE increased by 500%, 1300% and 3200% approximately. Because the carbonyl iron particles can form chain-like aggregation structure along the fibre directions, the conductivity of the FFW–MRE showed a typical anisotropic characteristic and it was sensitive to the external stimulus. When the compressive direction was parallel to the fibre weaves, the resistance of the FFW–MRE reduced to 2.7 kΩ, which was only 1/71 of the pure MRE. A possible mechanism was proposed to investigate in detail mechanical and electrical properties of the FFW–MRE. This method provides an economical, effective and environmentally friendly way to improve shear properties, compressive properties, tensile properties and conductivity of MREs.

Keywords: magnetorheological elastomer, fibre weaves, mechanical property, conductivity

(Some figures may appear in colour only in the online journal)

1. Introduction

Magnetorheological elastomer (MRE) is a kind of smart material which is usually prepared by dispersing magnetic iron particles into the polymer matrix. When the external magnetic field is applied onto the MREs, the magnetic particles interact with the matrix thus the mechanical properties can be precisely controlled by the external stimulation. Due to this unique magnetorheological behaviour, the MREs possessed wide application in vibration control, architecture, noise reduction etc [1–7]. It was reported that the isolation/adsorption frequency of the MRE based device were mainly dependent on the mechanical properties of the MRE. Therefore, most of the previous works were focused on improving the mechanical and magnetorheological properties of MREs so as to meet the requirements in practical application [8–12].

The polymer matrix is very important for the mechanical performance of the MREs. Besides the traditional natural rubber [12] and silicone rubber [13], the gel [14–17], sponge [18, 19] and silly putty [20] have also been used as the matrix to enhance the magnetorheological effect. It was found that gel and silly putty could greatly enlarge the magnetic-induced normal force, and the magnetic-induced modulus of sponge-based MRE was increased significantly. Moreover, by varying the cross-link density of the polymer, the damping properties of the MRE was controllable [21, 22]. Recently, many efforts were conducted to enlarge the MR performance by introducing the MRE with functional additives. For example, due to the phase-change characteristic of the poly (lactic acid) (PLA) doping, the PLA-MRE presented an

[1] Authors to whom any correspondence should be addressed.

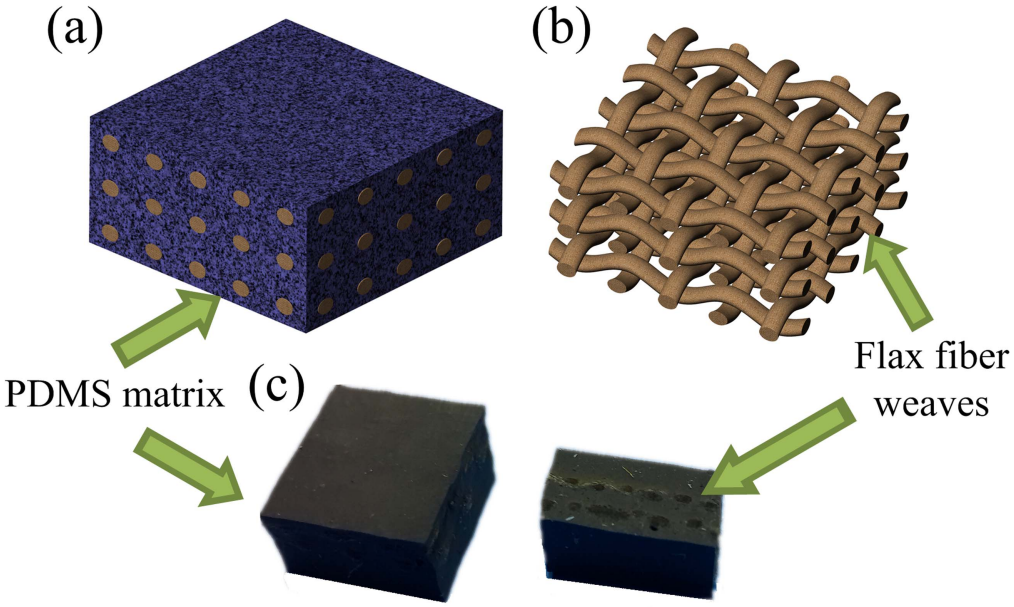

Figure 1. The schematic of MRE (a) with fibre weaves (b) and the photo of MREs (c).

unusual temperature-dependent mechanical behaviour [23]. Yu *et al* [24] embedded copper coil into the MRE to improve the field-dependent properties. Ubaidillah *et al* [25, 26] successfully took advantage of the waste tire rubber to fabricate MRE through the process of formation–destruction–reformation of the internal network. The elastomer which has the ability to support and recover still plays an important role in applications. In practical vibration control applications, the MRE located in the adaptive sandwich structures [27–32] should exhibit high anti-loading, MR effect, and recovery performance. To meet the above requirements, various additives such as the silicon carbide [33], carbon black [34], carbon nanotube [35], etc were used to reinforce the MRE.

Flax fibre is often used for improving mechanical properties of the polymer matrix [36–40]. Although it is lighter than the glass fibre, its stiffness is high (30–70 GPa). Interestingly, different from the traditional fibre, the flax fibre could be weaved and the flax-fibre-weaves (FFWs) were effective for improving the strength and crack-resistant properties of the biocomposite sheets [41]. Bos *et al* [42] developed a novel flax/polypropylene compounds and found that flax fibres improved the strength and stiffness by reaching the compatibilisation of the fibre/matrix interphase. To this end, the FFW will be a suitable candidate for strengthening the MRE. Moreover, the conductive MRE has drawn more and more attention because its resistance could respond to the external strain or magnetic field [43–46]. In consideration of the 2D structure of the FFWs, the conductive carbonyl iron (CI) particles would form conductive path through attaching onto the flax fibres. Therefore, the introducing of the FFWs into MRE will both improve mechanical and electrical performance.

In this study, we reported a novel FFW strengthened MRE and investigated its rheological properties, compressive properties, tensile properties, and electrical performances. The influence of loading directions, density and layer numbers of the FFWs on the mechanical and electrical properties of the FFW–MRE were studied. Besides, the mechanisms of structure formation and enhancement performance were discussed. Since the simplicity of the fabricating process and highly improved performance, it is a potential method to broaden the practical applications of MREs.

2. Experimental section

2.1. Preparation of MREs

In this study, polydimethylsiloxane (PDMS) (Dow Corning GmbH, USA) was selected as the matrix [47], and the Sylgard 184 was selected as vulcanizer. PDMS was selected as the matrix because it was liquid before curing. The liquid matrix could be easily fulfilled into the gaps in the single strand of fibre, and it exhibited good compatibility to FFWs. Besides, due to the addition of FFWs, many bubbles appeared around the FFWs during the preparation. It was difficult to remove bubbles when nature rubber was used. If the high temperature was applied to remove bubbles, MRE would be cured. In addition, PDMS could provide high elasticity and stability. Above all, PDMS was chosen as the matrix of MRE in this study. The magnetic particles were (CI, type CN) with an average diameter of 6 μm produced by BASF. In order to enhance shear mechanical properties, different types of flax fibre weaves (Jiujiang Yarnfan Textile Co. Ltd, China) were added into the matrix, with 4, 5, 6, or 7 strands of fibre per centimeter. The formation schematic of FFW–MRE was shown in figure 1.

In order to directly study the effects of flax fibre on MRE's mechanical and electrical properties, no conductive additive except CI particle was added in the MREs. PDMS, Sylgard 184 and CI power were mixed homogeneously in a beaker, and then the mixture was transferred into a vacuum oven to

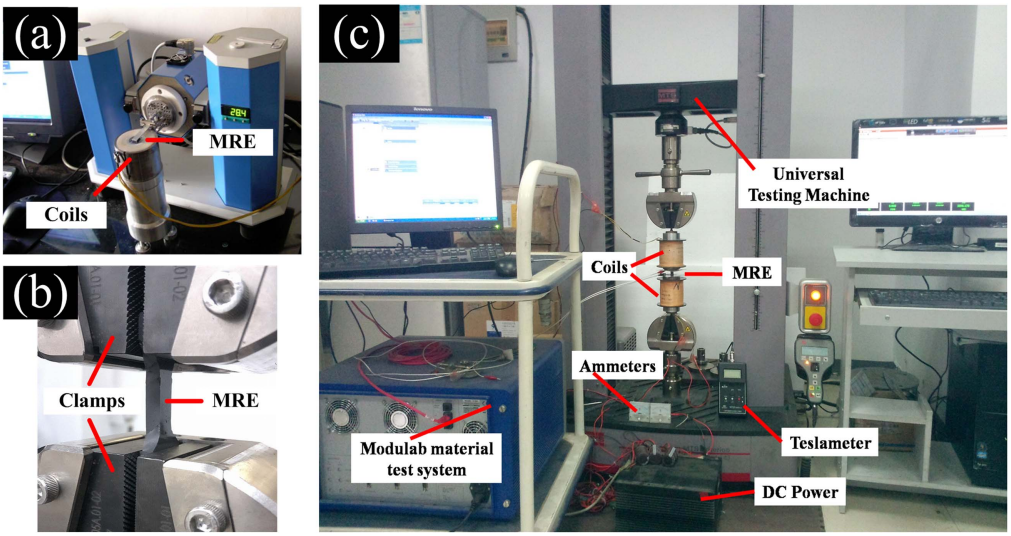

Figure 2. The modified dynamic mechanical analyser (a), the clamps of electromechanical universal testing machine (b) and the electrical test system (c).

eliminate air bubbles for 15 min. A certain quality of CI particles were scattered on the flax fibres to match the mass fraction of CI in MRE, and promote the particles' attachment and distribution. After that, the mixture was poured into the mould and the flax fibre weaves parallel to the mould were located within the PDMS/CI mixture. After pumping for another 15 min, the mixture was compressed tightly and cured under 100 °C for 30 min. In this research, the dimensions of MRE samples for dynamic mechanical tests, quasi-static compressive tests and electrical tests were 5 mm × 5 mm × 5 mm, and the MREs in the quasi-static tensile tests were cut into dumbbell-shaped, with 20 mm length, 10 mm wide and 5 mm thick in the centre stretched area.

2.2. Test system and methods

The morphology of MRE samples were characterized by an environment scanning electron microscopy (SEM, Philips of Holland, model XL30 ESEM-TMP), operating at 20.0 kV. Each sample was cut into flakes and coated with a thin layer of gold for observation.

MRE's dynamic mechanical performance was measured by a modified dynamic mechanical analyser (DMA, Triton Technology Ltd, UK, model Tritec 2000B) (figure 2(a)). A self-made electromagnet, which could generate a variable magnetic field from 0 to 800 mT, was attached to the DMA. The testing frequency swept from 1 to 19 Hz, and the shear strain amplitude was set at 0.1%.

The electromechanical universal testing machine (Model 43, MTS System Corporation, China) was used to quasi-statically load tension (figure 2(b)) and compression (figure 2(c)). It was controlled by the computer and the relationship between force and displacement was measured. The strain was loaded from 0% to 20% in compression tests and from 0% to 10% in tensile tests. The compressive or tensile frequency was 0.05 Hz. After fixing the magnetic field generators (which could generate a variable magnetic field from 0 to 400 mT) with the clamps, MRE could be loaded under magnetic field and compression at the same time.

The Modulab material test system (MTS, Solartron Analytical, AMETEK Advanced Measurement Technology, Inc., United Kingdom) (figure 2(c)) was used to test the electrical property. It could supply direct voltage excitation and measured the responsive current. The DC voltage excitation was set at 6 V. The conductive adhesive tape (Suzhou Crystal Electronic Technology Co. Ltd, China) was used to link the MRE and the polished copper plates, and two signal lines were used to connect copper polar plates and the Modulab MTS. The gap between the coils and the intensity of current were adjusted constantly, so we used a teslameter (type HT20, Shanghai Hengtong magnetic technology Co. Ltd, China) to measure the magnetic flux density.

3. Result and discussion

3.1. Microstructure of the FFW–MREs

Figure 3(a) shows the SEM image of pure MRE with CI particle content of 50 wt%. The white CI particles were randomly distributed in the black PDMS matrix. Interestingly, once the FFW was added into the MRE, the inner structure was critically changed. As shown in figure 3(b) was the cross-sectional microstructures of FFW–MREs in the direction of vertical to the flax fibre layers. The PDMS matrix was liquid before vulcanization, thus the gap among the single strand of fibre could be fulfilled with the PDMS-based MRE (figure 3(b)), which demonstrated the well combination between the matrix and the fibres. Large amount of CI particles was gathered in the vicinity of the flax fibre (figure 3(c)), which was because the roughness of the fibre surface was favoured for adsorbing particles. Furthermore, the CI particles were tightly located among the fibres after curing the matrix. Therefore, the flax fibre layer changed the aggregation structure of particles in the MREs. In this progress, although the magnetic field was not

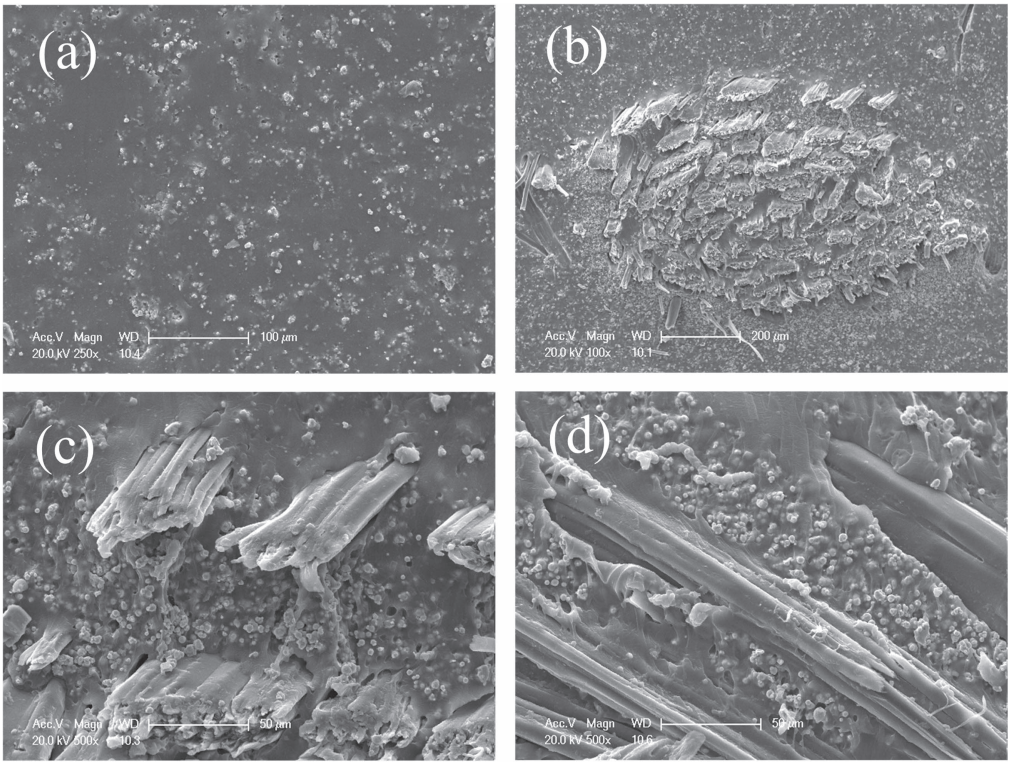

Figure 3. The SEM images of pure MRE (a) and FFW–MRE's cross section when perpendicular (b), (c) or parallel (d) to the FFW with CI particle content of 50 wt%.

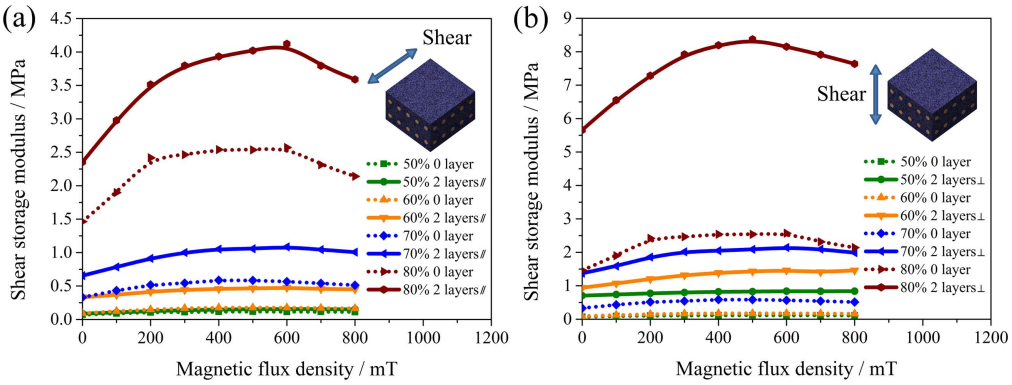

Figure 4. The shear storage modulus of FFW–MRE with different CI content when the shear direction was parallel (a) or perpendicular (b) to the fibre layers.

applied during vulcanization, the particles can still form a wire-like aggregation structure along the fibre directions. This convenient and environmental friendly method is easy to prepare thicker MREs with longer chain structures.

3.2. Shear performance of FFW–MREs

The figure 4 shows the magnetic flux density dependent shear storage modulus of FFW–MREs with different CI content and flax fibre layers. When the modulus increased, the stress relaxation happened at the same time. Under high magnetic flux density, the ferromagnetic particles reached the saturation magnetization, so at this time the stress relaxation played the major role in the change of modulus. On the other hand, the coil which produced magnetic field was constantly heating, which rose the MRE's temperature and reduced the particles' saturation magnetization. Therefore, the shear storage modulus decreased under high magnetic flux density. When the shear direction was parallel to the fibre layers, the storage modulus of the FFW–MRE with 50 wt% CI powder increased from 0.09 to 0.16 MPa with the increase of magnetic flux density, exhibited a typical MR effect. In comparison to the pure MRE, the storage modulus of the FFW–MRE was a little larger (figure 4(a)), which must be responded for the strengthening effect of the FFW. Here, with increasing of CI content and the fibres, and the storage modulus of the FFW increased. Interestingly, the shear direction had a critical influence on the storage modulus. When the shearing direction was perpendicular to the fibre layers (figure 4(b)), the enhancing effect of the FFWs was much larger than the case

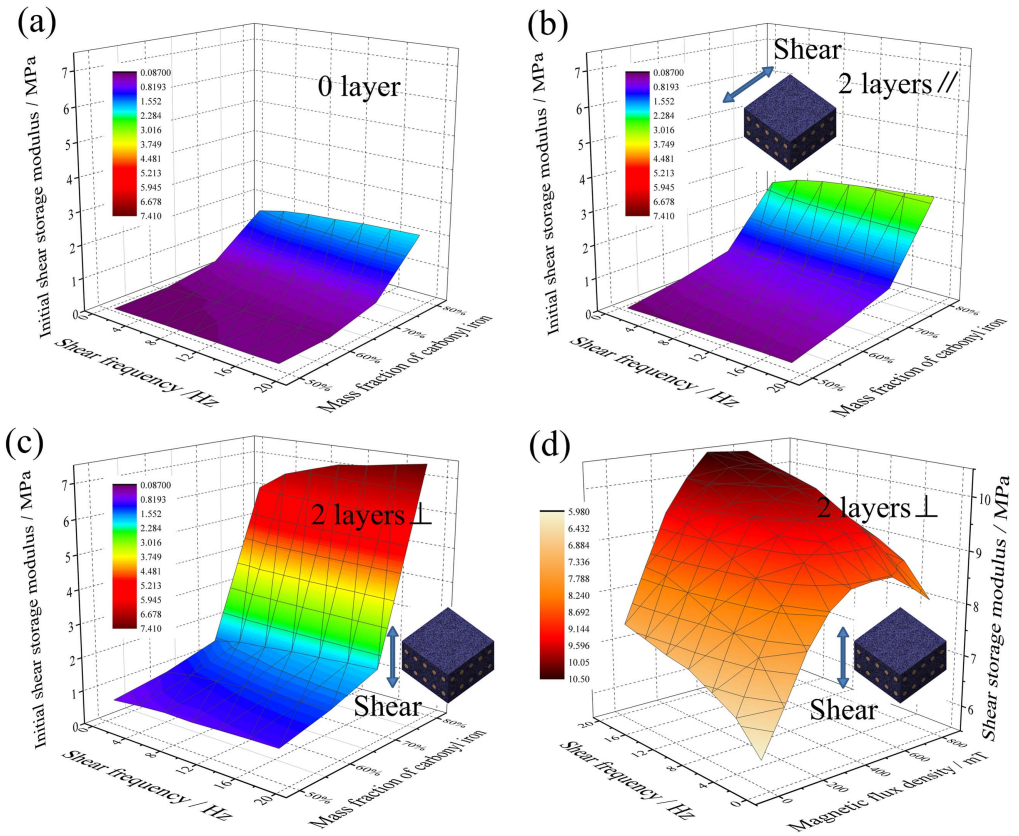

Figure 5. The initial storage modulus of MRE under different conditions: (a) without flax fibres; (b)–(d) with 2 flax fibre layers, the shear direction was parallel (b) or perpendicular (c), (d) to the fibre layers; (d) the mass fraction of CI was 80 wt%.

under the parallel direction. Typically, the storage modulus of FFW–MRE with 50 wt% CI content was higher than the pure MRE with 70 wt% CI content. The above mechanical behaviours of the FFW–MRE were similar to that of the MRE, whose CI chain-like structures were formed by pre-structure process under magnetic field without any fibres. So it also reflected that the CI particles can attach to the flax fibre surface or aggregate around to form chain-like structures, and FFWs greatly enhanced the shear storage modulus.

The dynamic mechanical properties of the FFW–MRE were tested by using a modified DMA. The shear frequency was swept from 1 to 19 Hz with strain amplitude of 0.1%. Here, the flax fibre layers with 5 strands per centimeter were selected for the FFW–MRE. Both the influence of flax fibre layers number and shear direction on the initial shear storage modulus of FFW–MRE was investigated (figure 5). In the absence of FFWs, the initial modulus increased slowly with increasing shear frequency and CI content. If the shear frequency was 1 Hz, the initial modulus increased from 0.09 to 1.5 MPa when the CI content increased from 50 to 80 wt% (figure 5(a)). For FFW–MRE with 2 layers of flax fibre, the initial storage modulus was improved obviously. When the shear direction was parallel to the FFWs, since the fibres did not structurally enhance the matrix in the shear direction, the friction between the rough fibres and the matrix played a major role on strengthening the interface. At 1 Hz, the initial modulus increased from 0.1 MPa (50 wt%) to 2.5 MPa (80 wt%) (figure 5(b)). When the shear direction was perpendicular to the fibre layers, due to the structural enhancement of the FFW, the storage modulus got a huge improvement. The initial modulus increased from 0.7 MPa (50 wt%) to 6.0 MPa (80 wt%) at 1 Hz (figure 5(c)) by varying the weight content of the CI particles. Besides, the effect of shear frequency was greatly enhanced at this time, the initial storage modulus reached 7.4 MPa at 19 Hz (80 wt%). In addition, as shown in figure 5(d), MRE also had obvious magnetorheological effect. In consideration of the mass of flax fibres per unit volume is far less than that of the iron particles, adding flax fibres is a convenient, economical and environmentally friendly way to improve the initial storage modulus of MRE.

The effects of density and layer numbers of FFW played important roles in determining the mechanical performance of the FFW–MRE. In this work, the inner characteristic of the FFW such as the spacing between adjacent fibres was also used to study the mechanical behaviour. Four kinds of FFWs with different density, which were woven by 4, 5, 6 and 7 strands of flax fibre per centimeter, were added into the MRE respectively. Figure 6 showed the comparison of the FFW–MRE prepared by different layers and kinds of flax fibre. Typically, with the increase of the layer numbers, the storage modulus of the FFW–MRE increased, indicated the strengthening effect. If the shear direction was parallel to the fibre layers (dash line), the increment of the storage modulus with the FFW was smaller as the fibres became denser. When the shear direction was perpendicular to the fibre layers (solid

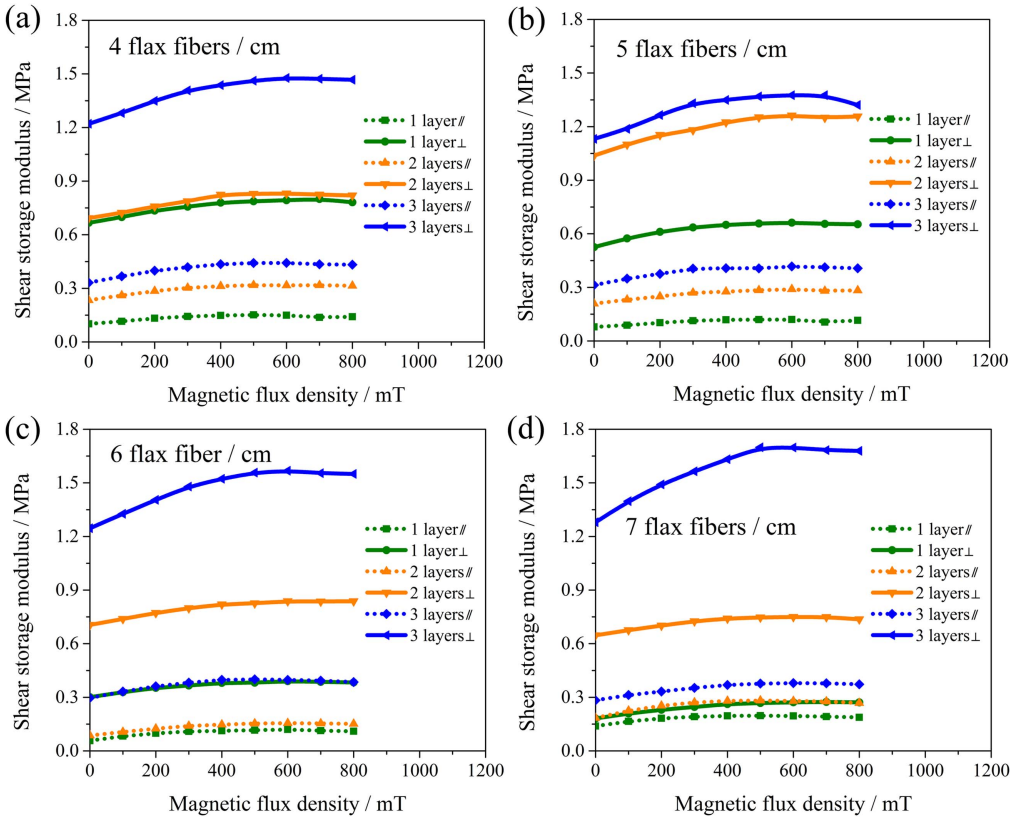

Figure 6. The storage modulus of MRE with different layers of FFW along the different shear directions with 50 wt% of CI: (a) 4 strands of fibre per centimeter; (b) 5 strands of fibre per centimeter; (c) 6 strands of fibre per centimeter; (d) 7 strands of fibre per centimeter.

line), for the single-layer structure, the initial storage modulus of the FFW–MRE contained 4, 5, 6 and 7 flax fibres per centimeter was 0.67 MPa, 0.53 MPa, 0.30 MPa and 0.18 MPa, respectively. So the interspace between the fibre layers is important for the mechanical performance of MREs. If the fibres were sparser, the storage modulus was higher. However, for the 3 layers' structure, the storage modulus was greatly enhanced, but the fibre density had little effect.

The enhancement of MRE's mechanical behaviour depended on not only the interfacial friction between the fibres and the matrix, but also the interaction between the fibre-bound matrix and the relatively free matrix (figure 12). The motion of the restrained rubber's molecular chain was bound, so the storage modulus of the restrained rubber was larger than that of the free rubber. Within a certain range, the sparser the flax fibres, the more restrained the matrix and the higher the MRE's modulus. In addition, after reached 3 layers, most of the matrix in the sample was subject to optimum restrains, so the storage modulus increased sharply, and the effects of fibre density appeared to be not obvious. While the shear direction was parallel to the fibre layers, the interlayer free matrix was the main factor for the small influence on the storage modulus.

The magneto-induced storage modulus is defined as $\Delta G = G - G_0$. Here G_0 is the initial storage modulus, and G is the storage modulus under different magnetic field. Through calculation and extraction, the magneto-induced storage modulus of the MRE with different layers and interval of flax fibre was obtained (figure 7). At this time, the content of the CI powder was 50 wt%. On the one hand, because the iron particles aggregated along the fibre direction to form particle chain structures, the magneto-induced modulus was greatly enhanced. On the other hand, the rough flax fibre strengthened the matrix structure and increased the initial modulus. As a consequence, the magnetorheological effect was not very high despite the magneto-induced modulus varied considerably.

For the sparsest FFWs of 4 strands per centimeter and the densest ones of 7 strands per centimeter, there was little difference in the magneto-induced modulus for the final FFW–MRE when the layer number of the FFWs was smaller than 2 (figures 7(a), (d)). When only one layer of FFWs was added into the MRE, the FFWs with 7 strands per centimeter lead to a magnetic-induced modulus of 0.10 MPa, which was a little less than the one prepared by 4 strands per centimeter FFWs (0.14 MPa). Therefore, a certain degree of fibre spacing was favourable to increase the restrained matrix, and the volume of the particle chains formed around the fibres. However, if the 3 layers of FFWs were used, the magneto-induced modulus of FFW–MREs with 4, 5, 6 and 7 fibres per centimeter was 0.26 MPa, 0.27 MPa, 0.34 MPa and 0.42 MPa, respectively. The rate of increase was also growing. Compare with the case of a single layer, the small spacing between adjacent fibre layers in multi-layer fibre structures was beneficial for particles in the interlayer of the fibres to be bound and aggregated.

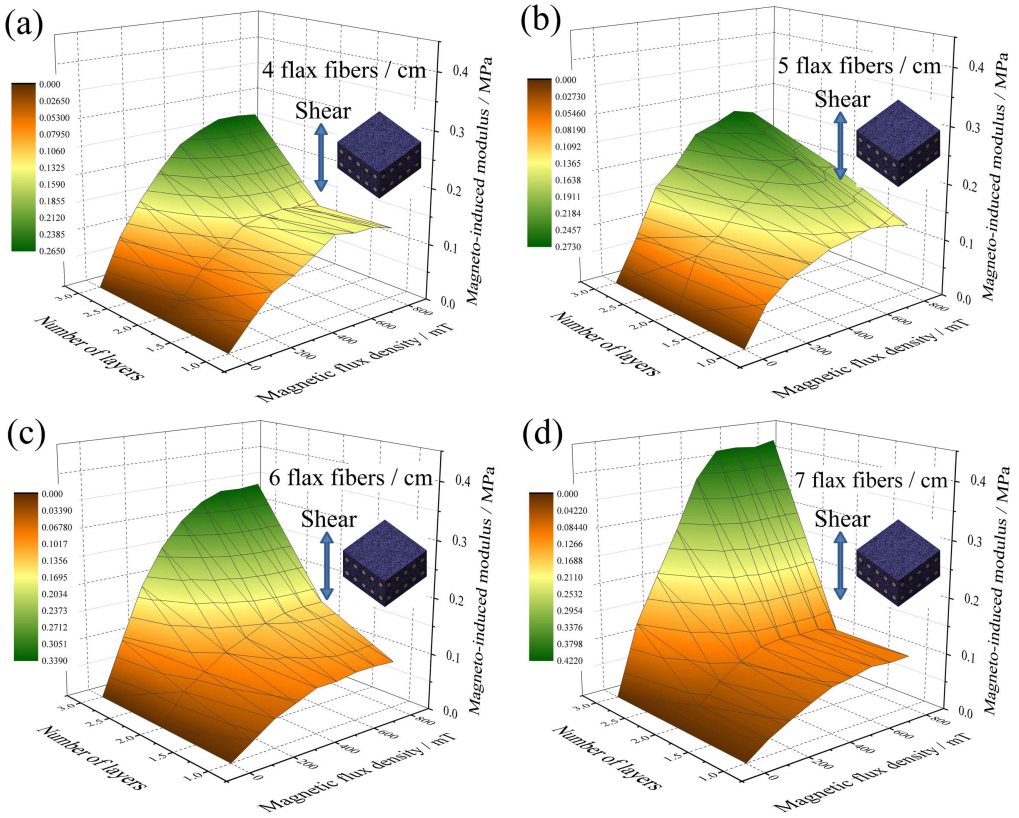

Figure 7. The magneto-induced storage modulus of MRE with different layers of flax fibre in the vertical direction with 50 wt% of CI: (a) 4 strands of fibre per centimeter; (b) 5 strands of fibre per centimeter; (c) 6 strands of fibre per centimeter; (d) 7 strands of fibre per centimeter.

3.3. Compressive and tensile performance of FFW–MREs

Because MREs often works under compression or vibration, the plastic deformation of the matrix is always a serious problem that affects the material's properties and life. Therefore, it is necessary to strengthen the matrix under the premise of ensuring MRE's performance. To investigate the quasi-static compressing behaviour of the MRE, the electronic universal testing machine was used. The compressive frequency was set as 0.05 Hz, and the strain amplitude was set as 20%. For pure MRE, when the CI content was 50 wt%, 60 wt%, 70 wt% and 80 wt%, the stress at 20% strain was 0.38 MPa, 0.39 MPa, 0.52 MPa and 0.94 MPa, respectively. When two flax fibres layers were added, the stress had an obvious increase. For instance, the stress already reached 0.93 MPa when the CI content was only 60 wt% if the compressive direction was perpendicular to the fibre layers in the FFW–MRE (figure 8(b)). At this time, more matrixes restrained by fibres, and resulted in the greater increase of the modulus than simply relying on the interaction between particles and matrix. If the compressive direction was parallel to the fibre layers, the matrix was structurally reinforced. Especially when the CI content was as high as 80 wt%, fibres were filled with more iron particles, so the modulus rose greater and reached 2.16 MPa (figure 8(c)). If the CI content was kept at 50 wt%, the fibre structure was more effective on matrix reinforcement than the particles after comparing with figure 8(a). This result indicated that this method not only ensured high shear modulus in the shear direction to the fibre layers, but also provided greater Young's modulus in compressive direction, which would be very useful and necessary in the field of vibration control.

In consideration of the PDMS matrix was strengthened by fibres, the magneto-induced effect of CI would be not obvious under magnetic field with low particle content, so MRE with 80 wt% CI content was selected (figure 9). The compressive frequency was also set as 0.05 Hz. As the magnetic flux density and the attraction of two magnetic poles were constantly changing during compression, the magnetic-field-induced stress has been deducted in calculating the stress. It was found that when the fibre layers were absent, the stress had a rising trend with the increase of magnetic flux density. After the strain reached 20%, the stress was 0.94 MPa, 0.99 MPa, 1.06 MPa, 1.10 MPa and 1.13 MPa when the magnetic flux density was 0 mT, 100 mT, 200 mT, 300 mT and 400 mT, respectively. When doped with two layers of fibre, the increase of stress with the magnetic flux density was not obvious. In addition, the difference of stress at maximum strain was small. This phenomenon further reflected the constraints of the fibres on the matrix and the particles. The area enclosed by the curve in figure 9(b) was significantly larger than that in figure 9(a), reflecting more energy was absorbed. This was also mainly due to the friction between the fibres and the matrix.

Under tensile conditions, the flax fibre layers also significantly improved the strength of the materials. The MRE samples were cut into dumbbell-shaped, with 20 mm length,

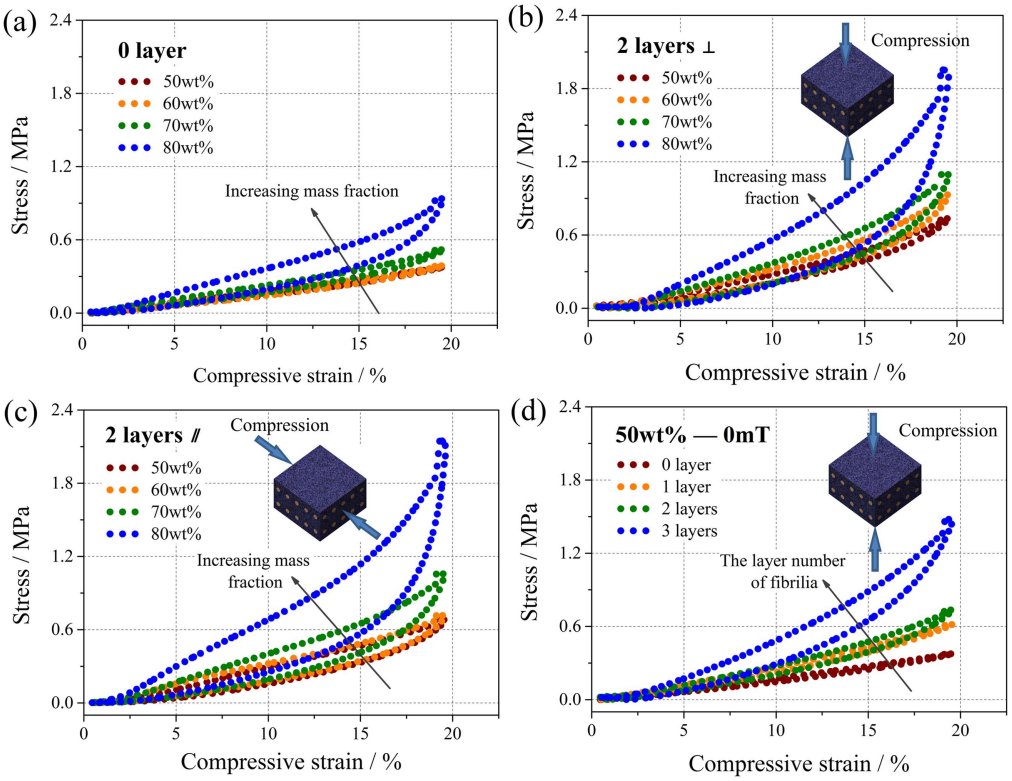

Figure 8. Stress–strain curves of MREs with different CI content under different compressive conditions: (a) without flax fibre layers; (b), (c) with 2 flax fibre layers, the shear direction was perpendicular (b), (d) or parallel (c) to the fibre layers; (d) the mass fraction of CI was 50 wt%.

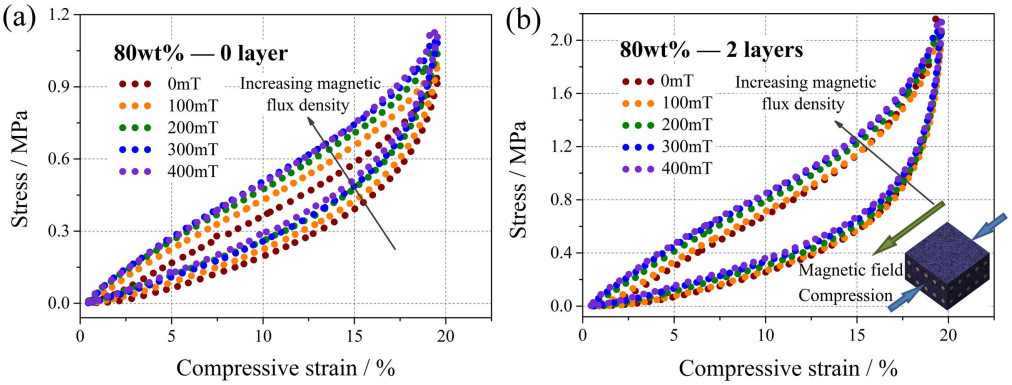

Figure 9. Stress–strain curves of MREs with 80 wt% CI content under different magnetic flux density: (a) without flax fibre layers; (b) with 2 flax fibre layers, the compressive direction was parallel to the fibre layers.

10 mm wide and 5 mm thick in the centre area. The tensile direction was parallel to the fibre layers. With 0 layer of flax fibre and 50 wt% of CI, the stress only reached 0.09 MPa at 10% strain. However, after 1, 2 and 3 layers of fibre were added, the tensile strength increased by 500%, 1300% and 3200% approximately (figure 10(a)). The good combination of the matrix and fibres could effectively improve the tensile strength. With increasing of the CI content, the strength of the MRE had a corresponding increase. And the higher the CI content, the greater the strength enhanced (figure 10(b)). However, when the CI content reached 70 wt% or even 80 wt%, the stress–strain curves fluctuated when the strain was about 5%. This is due to the relative displacement, caused by exceeding the upper limit of the surface stiction, happened between the matrix and the fibre (figure 12). The content of the particles was large at this time, and the particles existing on the fibre surface promote the relative displacement on the interface.

3.4. Conductivity of FFW–MREs

The electrical performance of MRE has now become a research hotspot due to its potential application in sensors. Here, due to the presence of flax fibres, the particle aggregation structures became order along with the FFWs, thus the conductivity of the MRE increased a the direction of the fibre

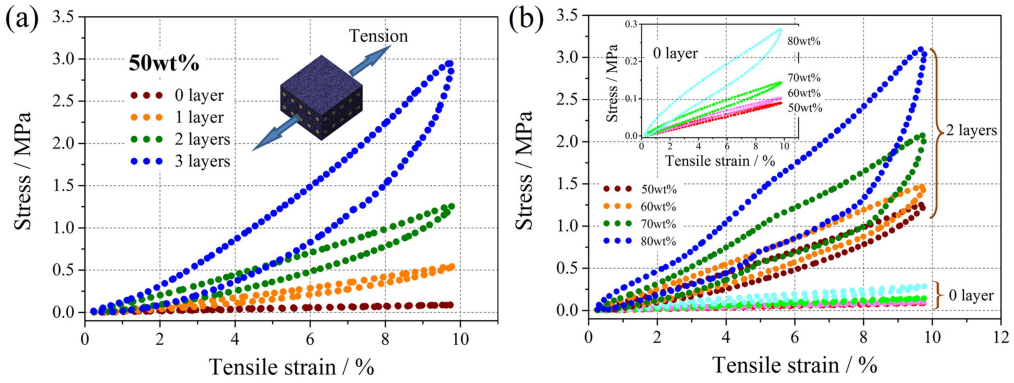

Figure 10. Stress–strain curves of MREs under quasi-static tensile conditions: (a) with different flax fibre layers, the CI content was 50 wt%; (b) with 0 or 2 layers of flax fibre, and different CI content. The tensile direction was parallel to the fibre layers.

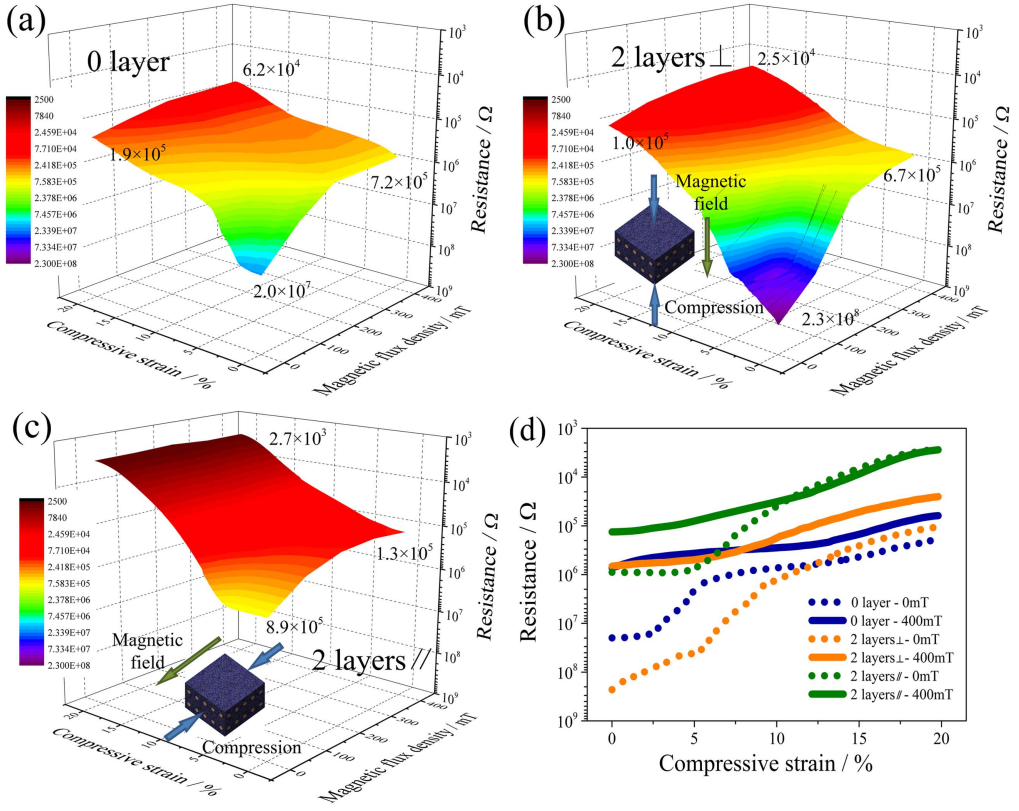

Figure 11. The resistance of MRE under different external stimuli with 80 wt% of CI: (a) without flax fibre layers; (b), (c) with 2 flax fibre layers, the compressive direction was perpendicular (b) or parallel (c) to the fibre layers; (d) under 0 and 400 mT of magnetic flux density.

layers (figure 11). The 2 layer FFWs strengthened MRE with 80 wt% CI was prepared in this experiment. As shown in figures 11(b) and (c), when the conductive direction was parallel or perpendicular to the 2 layers of fibre, the resistance achieved $8.9 \times 10^5\ \Omega$ or $2.3 \times 10^8\ \Omega$ without applied any strain, which was 0.05 or 11.6 times of the pure MRE's (figure 11(a)), respectively. The particle-attached aggregation structure in the direction of the fibre layers played a great role in the circuit's breakover, and the non-conductive flax fibre in the perpendicular direction to the fibre layers played a great role of insulation. Therefore, the electrical properties of FFW–MRE were anisotropic (figure 12).

In addition, the conductivity of the FFW–MRE had a significant response to the magnetic field and compressive strain (figure 11(d)). For MREs, the nonlinearity under different magnetic flux density is mainly due to the nonlinearity relationship between the interparticle conductivity and the spacing between particles. When MRE was under 400 mT, the spacing between particles is smaller than the one under 0 mT, so the first half of curves under 400 mT corresponded to the second half of the curves under 0 mT. In the direction of fibre layers, when the strain reached 20%, the resistance was even as low as 2.7 kΩ, which was only 1/71 of the case without fibres. And in the perpendicular direction to the fibre

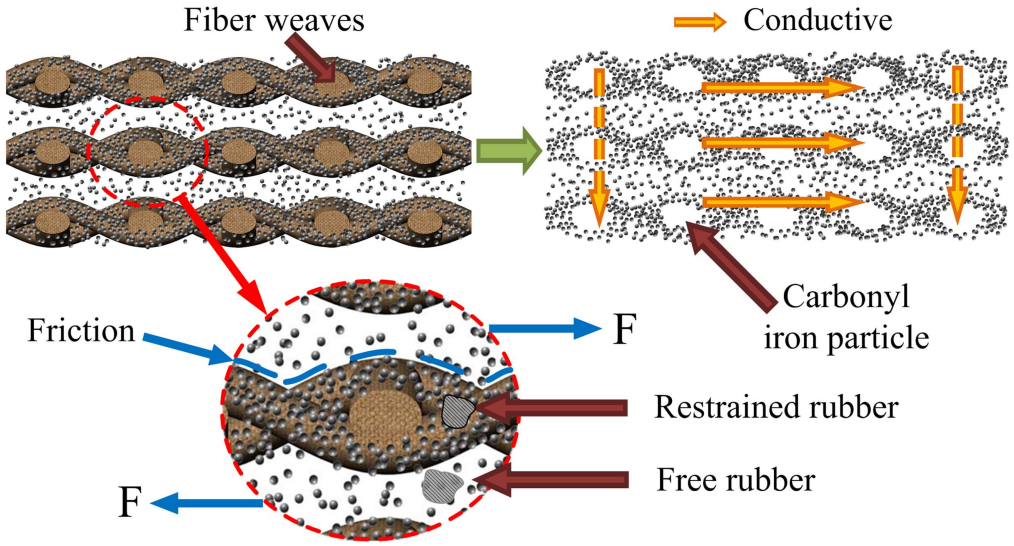

Figure 12. The sketch of the distribution of particles with FFW, and the mechanism of conductivity and mechanical properties.

layers, the distance between the particles aggregated around the fibre decreased rapidly under the magnetic field and pressure, so the resistance transformed from smaller to larger than that without the fibre layers. The above-mentioned anisotropic electrical properties, can not only improve the sensing ability in one direction, but also improve insulation in the other direction perpendicular. The adjustable range of the resistance was greatly improved by the stimulation of pressure or magnetic field. The linearity does not preclude the FFW–MRE from being a kind of potential sensor materials. This problem can be solved by selecting a linear segment, or by using a non-linear scale, or by designing a nonlinear compensation for the circuit.

4. Conclusion

In this work, we developed an FFW doping method to strengthen shear properties, compressive properties, tensile properties and conductivity of the PDMS based MREs. The gap among the strands of fibres could be well filled with the PDMS-based MRE and the matrix combined well with the fibres, thus both the layers' number and inner structure characteristic of the FFWs affected the final mechanical behaviour. The CI particles can form aggregation structure along the fibre direction through this method, which is more convenient and environmental friendly in the industry. When the shear direction was perpendicular to the fibre layers, FFW–MRE had a structural enhancement in the shear direction. The more the CI content, the stronger the reinforcing effect of the fibres on the matrix. The enhancement of MRE's mechanical behaviour not only depended on the interfacial friction between the fibres and the matrix, but also on the interaction between the fibre-bound matrix and the relatively free matrix. The storage modulus of the restrained rubber was larger than that of the free rubber. Because of the particles' aggregation structures along the fibre direction, the magneto-induced modulus was greatly enhanced. When the MREs were under compression or tension, FFW significantly improved the strength of the materials. The fibre structures were more effective on matrix reinforcement than the particles. Due to the ordered particle aggregation structure, the conductivity of the MRE increased when parallel to the direction of the fibre layers. In the direction of fibre layers, when the strain reached 20%, the resistance was even as low as 2.7 kΩ, which was only 1/71 of the case without fibres. In the vertical direction, insulation and adjustable range of resistance were greatly improved.

Acknowledgments

Financial supports from the National Natural Science Foundation of China (Grant No. 11572309, 11572310), the Strategic Priority Research Program of the Chinese Academy of Sciences (Grant No. XDB22040502), and the Fundamental Research Funds for the Central Universities (WK2480000002) are gratefully acknowledged. This study was also supported by the Collaborative Innovation Center of Suzhou Nano Science and Technology, and National Synchrotron Radiation Laboratory (University of Science and Technology of China).

References

[1] Choi S B, Li W H, Yu M, Du H P, Fu J and Do P X 2016 State of the art of control schemes for smart systems featuring magneto-rheological materials *Smart Mater. Struct.* **25** 043001
[2] Fu J, Li P D, Wang Y, Liao G Y and Yu M 2016 Model-free fuzzy control of a magnetorheological elastomer vibration isolation system: analysis and experimental evaluation *Smart Mater. Struct.* **25** 035030
[3] Fu J, Liao G Y, Yu M, Li P D and Lai J J 2016 NARX neural network modeling and robustness analysis of magnetorheological elastomer isolator *Smart Mater. Struct.* **25** 125019

[4] Gu X Y, Li Y C and Li J C 2016 Investigations on response time of magnetorheological elastomer isolator for real-time control implementation *Smart Mater. Struct.* **25** 11LT04

[5] Sun S S, Yang J, Li W H, Deng H X, Du H P, Alici G and Yan T H 2016 An innovative MRE absorber with double natural frequencies for wide frequency bandwidth vibration absorption *Smart Mater. Struct.* **25** 055035

[6] Yang J, Sun S S, Tian T F, Li W H, Du H P, Alici G and Nakano M 2016 Development of a novel multi-layer MRE isolator for suppression of building vibrations under seismic events *Mech. Syst. Signal Process.* **70-71** 811–20

[7] Gu X Y, Li J C, Li Y C and Askari M 2016 Frequency control of smart base isolation system employing a novel adaptive magneto-rheological elastomer base isolator *J. Intell. Mater. Syst. Struct.* **27** 849–58

[8] Malecki P, Krolewicz M, Hiptmair F, Krzak J, Kaleta J, Major Z and Piglowski J 2016 Influence of carbonyl iron particle coating with silica on the properties of magnetorheological elastomers *Smart Mater. Struct.* **25** 105030

[9] Pickering K L, Khimi S R and Ilanko S 2015 The effect of silane coupling agent on iron sand for use in magnetorheological elastomers: I. Surface chemical modification and characterization *Composites* A **68** 377–86

[10] Chen D, Yu M, Zhu M, Qi S and Fu J 2016 Carbonyl iron powder surface modification of magnetorheological elastomers for vibration absorbing application *Smart Mater. Struct.* **25** 115005

[11] Khimi S R and Pickering K L 2016 The effect of silane coupling agent on the dynamic mechanical properties of iron sand/natural rubber magnetorheological elastomers *Composites* B **90** 115–25

[12] An J S, Kwon S H, Choi H J, Jung J H and Kim Y G 2017 Modified silane-coated carbonyl iron/natural rubber composite elastomer and its magnetorheological performance *Compos. Struct.* **160** 1020–6

[13] Bunoiu M and Bica I 2016 Magnetorheological elastomer based on silicone rubber, carbonyl iron and Rochelle salt: effects of alternating electric and static magnetic fields intensities *J. Ind. Eng. Chem.* **37** 312–8

[14] Mordina B, Tiwari R K, Setua D K and Sharma A 2016 Impact of graphene oxide on the magnetorheological behaviour of $BaFe_{12}O_{19}$ nanoparticles filled polyacrylamide hydrogel *Polymer* **97** 258–72

[15] Xu Y G, Liao G J, Zhang C Y, Wan Q and Liu T X 2016 The transition from stress softening to stress hardening under cyclic loading induced by magnetic field for magneto-sensitive polymer gels *Appl. Phys. Lett.* **108** 161902

[16] Yu M, Ju B X, Fu J, Liu S Z and Choi S B 2014 Magnetoresistance characteristics of magnetorheological gel under a magnetic field *Ind. Eng. Chem. Res.* **53** 4704–10

[17] Ju B X, Yu M, Fu J, Zheng X and Liu S Z 2013 Magnetic field-dependent normal force of magnetorheological gel *Ind. Eng. Chem. Res.* **52** 11583–9

[18] Ge L, Xuan S H, Liao G J, Yin T T and Gong X L 2015 Stretchable polyurethane sponge reinforced magnetorheological material with enhanced mechanical properties *Smart Mater. Struct.* **24** 037001

[19] Ge L, Gong X L, Wang Y and Xuan S H 2016 The conductive three dimensional topological structure enhanced magnetorheological elastomer towards a strain sensor *Compos. Sci. Technol.* **135** 92–9

[20] Guo F, Du C B, Yu G J and Li R P 2016 The static and dynamic mechanical properties of magnetorheological silly putty *Adv. Mater. Sci. Eng.* **2016** 7079698

[21] Fan Y C, Gong X L, Xuan S H, Qin L J and Li X F 2013 Effect of cross-link density of the matrix on the damping properties of magnetorheological elastomers *Ind. Eng. Chem. Res.* **52** 771–8

[22] Aloui S and Kluppel M 2015 Magneto-rheological response of elastomer composites with hybrid-magnetic fillers *Smart Mater. Struct.* **24** 025016

[23] Tanrattanakul V and Bunkaew P 2014 Effect of different plasticizers on the properties of bio-based thermoplastic elastomer containing poly(lactic acid) and natural rubber *Express Polym. Lett.* **8** 387–96

[24] Yu M and Wang S Q 2010 The composite MRE embedded with a copper coil *Smart Mater. Struct.* **19** 065023

[25] Ubaidillah, Choi H J, Mazlan S A, Imaduddin F and Harjana 2016 Fabrication and viscoelastic characteristics of waste tire rubber based magnetorheological elastomer *Smart Mater. Struct.* **25** 115026

[26] Ubaidillah, Imaduddin F, Li Y C, Mazlan S A, Sutrisno J, Koga T, Yahya I and Choi S-B 2016 A new class of magnetorheological elastomers based on waste tire rubber and the characterization of their properties *Smart Mater. Struct.* **25** 115002

[27] Eshaghi M, Sedaghati R and Rakheja S 2016 Dynamic characteristics and control of magnetorheological/electrorheological sandwich structures: a state-of-the-art review *J. Intell. Mater. Syst. Struct.* **27** 2003–37

[28] Babu V R and Vasudevan R 2016 Dynamic analysis of tapered laminated composite magnetorheological elastomer (MRE) sandwich plates *Smart Mater. Struct.* **25** 035006

[29] Kozlowska J, Boczkowska A, Czulak A, Przybyszewski B, Holeczek K, Stanik R and Gude M 2016 Novel MRE/CFRP sandwich structures for adaptive vibration control *Smart Mater. Struct.* **25** 035025

[30] Yildirim T, Ghayesh M H, Li W H and Alici G 2016 Experimental nonlinear dynamics of a geometrically imperfect magneto-rheological elastomer sandwich beam *Compos. Struct.* **138** 381–90

[31] Yildirim T, Ghayesh M H, Li W H and Alici G 2016 An experimental investigation into nonlinear dynamics of a magneto-rheological elastomer sandwich beam *Smart Mater. Struct.* **25** 015018

[32] Yildirim T, Ghayesh M H, Li W H and Alici G 2016 Nonlinear dynamics of a parametrically excited beam with a central magneto-rheological elastomer patch: an experimental investigation *Int. J. Mech. Sci.* **106** 157–67

[33] Wang Y, Gong X L, Yang J and Xuan S H 2014 Improving the dynamic properties of MRE under cyclic loading by incorporating silicon carbide nanoparticles *Ind. Eng. Chem. Res.* **53** 3065–72

[34] Nayak B, Dwivedy S K and Murthy K S R K 2015 Fabrication and characterization of magnetorheological elastomer with carbon black *J. Intell. Mater. Syst. Struct.* **26** 830–9

[35] Aziz S A A, Mazlan S A, Ismail N I N, Ubaidillah U, Choi S B, Khairi M H A and Yunus N A 2016 Effects of multiwall carbon nanotubes on viscoelastic properties of magnetorheological elastomers *Smart Mater. Struct.* **25** 077001

[36] Bos H L, Van den Oever M J A and Peters O C J J 2002 Tensile and compressive properties of flax fibres for natural fibre reinforced composites *J. Mater. Sci.* **37** 1683–92

[37] Sanadi A R, Caulfield D F, Jacobson R E and Rowell R M 1995 Renewable agricultural fibers as reinforcing fillers in plastics—mechanical-properties of kenaf fiber-polypropylene composites *Ind. Eng. Chem. Res.* **34** 1889–96

[38] Caulfield D F, Feng D, Prabawa S, Young R A and Sanadi A R 1999 Interphase effects on the mechanical and physical aspects of natural fiber composites *Angew. Makromol. Chem.* **272** 57–64

[39] Bos H L, Molenveld K, Teunissen W, van Wingerde A M and van Delft D R V 2004 Compressive behaviour of unidirectional flax fibre reinforced composites *J. Mater. Sci.* **39** 2159–68

[40] Mahboob Z, El Sawi I, Zdero R, Fawaz Z and Bougherara H 2017 Tensile and compressive damaged response in flax fibre reinforced epoxy composites *Composites* A **92** 118–33
[41] Wu Q, Rabu J, Goulin K, Sainlaud C, Chen F, Johansson E, Olsson R T and Hedenqvist M S 2017 Flexible strength-improved and crack-resistant biocomposites based on plasticised wheat gluten reinforced with a flax-fibre-weave *Composites* A **94** 61–9
[42] Bos H L, Mussig J and van den Oever M J A 2006 Mechanical properties of short-flax-fibre reinforced compounds *Composites* A **37** 1591–604
[43] Ghafoorianfar N, Wang X J and Gordaninejad F 2014 Combined magnetic and mechanical sensing of magnetorheological elastomers *Smart Mater. Struct.* **23** 055010
[44] Ausanio G, Iannotti V, Ricciardi E, Lanotte L and Lanotte L 2014 Magneto-piezoresistance in magnetorheological elastomers for magnetic induction gradient or position sensors *Sensors Actuators* A **205** 235–9
[45] Liu Y D and Choi H J 2013 Recent progress in smart polymer composite particles in electric and magnetic fields *Polym. Int.* **62** 147–51
[46] Bica I, Liu Y D and Choi H J 2012 Magnetic field intensity effect on plane electric capacitor characteristics and viscoelasticity of magnetorheological elastomer *Colloid Polym. Sci.* **290** 1115–22
[47] Li W H and Nakano M 2013 Fabrication and characterization of PDMS based magnetorheological elastomers *Smart Mater. Struct.* **22** 055035